Journal of Radiation Research and Applied Sciences 18 (2025) 101528

Contents lists available at ScienceDirect

Journal of Radiation Research and Applied Sciences

journal homepage: www.journals.elsevier.com/journal-of-radiation-research-and-applied-sciences

Radioactivity distribution in soil, rock and tailings at the Geita Gold Mine in Tanzania

Jerome M. Mwimanzi [a,b], Nils H. Haneklaus [a,c,d,*], Tomislav Bituh [e], Hendrik Brink [f], Katarzyna Kiegiel [g], Farida Lolila [h], Janeth J. Marwa [a,i], Mwemezi J. Rwiza [a], Kelvin M. Mtei [a]

[a] School of Materials Energy Water and Environmental Sciences, Nelson Mandela African Institution of Science and Technology, P.O. Box 442, Arusha, Tanzania
[b] Tanzania Atomic Energy Commission, P.O. Box 743, Arusha, Tanzania
[c] Td-Lab Sustainable Mineral Resources, Danube University Krems, University for Continuing Education, Dr.-Karl-Dorrek-Straße 30, 3500, Krems an der Donau, Austria
[d] Unit for Energy and Technology Systems - Nuclear Engineering, North-West University, 11 Hoffman Street, Potchefstroom, 2520, South Africa
[e] Institute for Medical Research and Occupational Health, Zagreb, Croatia
[f] Department of Chemical Engineering, University of Pretoria, Pretoria, 0002, South Africa
[g] Institute of Nuclear Chemistry and Technology, Dorodna 16, 03-195, Warsaw, Poland
[h] Facult of Science, Dar es Salaam University College of Education, P.O. Box 2329, Dar es Salaam, Tanzania
[i] School of Business Studies and Humanities, NM-AIST, P.O. Box 442, Arusha. Tanzania, Tanzania

ARTICLE INFO

Keywords:
Natural radioactivity
Radiological hazard indices
Gold mining
Tanzania

ABSTRACT

This study evaluated the activity concentrations of natural radionuclides in soil, waste rocks and tailings from the Geita gold mining site in Tanzania using high-resolution gamma spectroscopy. A total of 41 samples: 31 soil, 5 waste rock, and 5 tailing samples were collected around the mine to assess their radiological hazards. The average activity concentrations in soil were 54, 45 and 279 Bq kg^{-1} for ^{226}Ra, ^{232}Th and ^{40}K. In contrast, tailings exhibited higher activity concentrations of 70, 36 Bq kg^{-1} for ^{226}Ra and ^{232}Th, and significantly elevated levels of 877 Bq kg^{-1} for ^{40}K, while waste rocks showed intermediate values, with 66, 73 and 660 Bq kg^{-1} for ^{226}Ra, ^{232}Th and ^{40}K respectively. Radiological hazard indices were calculated to quantify potential risks. In soil, the radium equivalent activity (Ra_{eq}) averaged 139 Bq kg^{-1}, the annual effective dose equivalent (AEDE) was 78 μSv y^{-1}, the annual gonadal dose equivalent (AGDE) reached 430 μSv y^{-1}, and the excess lifetime cancer risk (ELCR) was 0.27 × 10^{-1}. Tailings showed a Ra_{eq} of 189 Bq kg^{-1}, AEDE of 111 μSv y^{-1}, AGDE of 678 μSv y^{-1}, and ELCR of 0.39 × 10^{-1}, while waste rocks exhibited a Ra_{eq} of 200 Bq kg^{-1}, AEDE of 108 μSv y^{-1}, AGDE of 642 μSv y^{-1}, and ELCR of 0.37 × 10^{-3}. Notably, the ELCR values for tailings and waste rocks exceeded the global average of 0.29 × 10^{-3}, rendering them unsuitable for use as building materials. The absorbed dose rates were 69 nGy h^{-1} for soil, 91 nGy h^{-1} for tailings, and 88 nGy h^{-1} for waste rocks. One-way ANOVA revealed significant differences ($p < 0.05$) among the matrices. These findings underscore the need for targeted waste management and remediation strategies to mitigate radiological health risks in the investigated mining area as well as other areas with similar characteristics.

1. Introduction

Naturally occurring radioactive material (NORM) is found throughout the Earth's crust with concentrations that vary depending on the local geology and geographical location (Michalik, Dvorzhak, & Pereira, 2023; Sumary et al., 2024). The International Atomic Energy Agency (IAEA) defines NORM in its glossary as "radioactive materials containing no significant amounts of radionuclides other than naturally occurring radionuclides" (Alharbi, 2024; IAEA, 2014, 2022). NORM primarily consist of uranium (^{238}U), thorium (^{232}Th), and potassium (^{40}K), along with their decay products including radium (^{226}Ra) (Kovler et al., 2017) and radon gas (Sawe, 2023). NORM is typically present in low levels in soil, water, plants, and air, posing minimal risk under natural conditions.

* Corresponding author. School of Materials Energy Water and Environmental Sciences, Nelson Mandela African Institution of Science and Technology, P.O. Box 442, Arusha, Tanzania.
E-mail address: nils.haneklaus@donau-uni.ac.at (N.H. Haneklaus).

https://doi.org/10.1016/j.jrras.2025.101528
Received 12 March 2025; Received in revised form 10 April 2025; Accepted 15 April 2025
Available online 30 April 2025

Anthropogenic activities, particularly those involving the extraction and processing of large quantities of minerals, as is the case in gold mining, are potential sources of NORM exposure. Despite the known risks, there is presently insufficient data on the radiological impact of large-scale gold mining in Tanzania, particularly concerning public exposure and environmental contamination. This lack of data hinders the development of an effective regulatory framework for radiation protection in mining communities. Long-term exposure to NORM may result in delayed health effects such as the development of certain forms of cancer such as leukemia (Doyi et al., 2016; Focus et al., 2021; ICRP, 2019).

Research across Africa, including Cameroon, Egypt, Ethiopia, Ghana, Kenya, Nigeria, and Tanzania, has shown that NORM activity concentrations vary widely. For instance, a study by Silver et al. (2016) in Southwestern Uganda identified elevated levels of NORM in mine tailings at the Mashonga Gold Mine. The absorbed dose rates were found to be three times higher than global averages, leading to recommendations against using these tailings as building materials. A similar study in South Africa reported high activity concentration of NORM in gold mines which exceeded the annual effective dose of 1 mSv per year limit set by the International Commission on Radiological Protection (ICRP, 2007). However, differences in methodologies and sample collection approaches make direct comparisons challenging. Previous studies in South Africa have investigated radiological hazards in mining environments (Kamunda et al., 2016; Moshupya et al., 2022). Faanu et al. (2011) and reported elevated NORM levels in soil, water, and vegetation were also reported at the Tarkwa gold mine in Ghana. These results are consistent with previous studies conducted in Ghana, Nigeria, and Uganda (Faanu et al., 2012; Odelami et al., 2024; Silver et al., 2016). However, unlike earlier studies, this research integrates geospatial mapping and statistical correlation analysis to offer a more comprehensive assessment of radiological risks in a large-scale mining environment (Rabuku & Malik, 2020; Tunde Ogundele et al., 2021).

Several studies have examined natural radioactivity in Tanzania (Banzi et al., 2017; Haneklaus, 2024; Kazoka, Mwalilino, & Mtoni, 2023; Lolila & Mazunga, 2023). However, most have focused on uranium mining areas, phosphates and small-scale gold mining. Limited research exists on radiation exposure from large-scale mining operations. This study addresses this gap in the literature by utilizing spatial mapping and statistical analysis to identify areas with elevated radiation levels, providing a more detailed assessment of potential risks to the public. Understanding the radiological risks associated with mining activities is essential for improving safety measures and environmental management practices. The results of this study will support the development of evidence-based radiation protection policies and help regulatory bodies determine the suitability of mine waste materials for various applications. Besides, this work will contribute to safeguarding public health and ensuring sustainable mining practices in Tanzania and other countries, particularly in Africa. A comprehensive assessment of these factors is essential to guide policy formulation, improve radiation protection measures, and mitigate potential environmental and health hazards. Specifically, this study evaluated the activity concentration of NORM in soil, waste rocks and tailings at the Geita gold mine (GGM) in Tanzania.

2. Materials and methods

2.1. Description of the study area

This study was conducted at the GGM in the Geita District of the Geita Region in Northwestern Tanzania. The GGM is one of the four largest operational mines in Tanzania, contributing substantially to both local and national economic development. The mine started operations in 1936 and remained active until 1966 when it ceased operations due to a financial crisis (Henckel et al., 2016). Following Tanzania's economic reforms the GGM resumed its operations in 2000 (Henckel et al., 2016). The mine employs open-pit and underground mining methods to optimize gold extraction based on the geological characteristics of the deposits (AngloGold, 2021). The mine is positioned at the headwaters of the Mtakuja River, which flows into Lake Victoria (Emel et al., 2014).

The main economic activities around the mine include farming, livestock keeping, and fishing. These activities are deeply intertwined with the mining operations, as the communities rely on both land use for agriculture and water from nearby sources, such as the Mtakuja River and Lake Victoria. Surrounding the mining site are six villages: Machinjioni, Mgusu, and Nyakabale in the Mgusu ward, and Mpomvu, Nyamalembo, and Samina situated in the Mtakuja ward, as shown in Fig. 1. These villages are directly influenced by the mining activities. The socio-economic impacts of mining extend beyond job opportunities and include significant concerns about environmental contamination, particularly regarding land use and access to clean water resources.

2.2. Geology of the study area

The GGM deposit is situated within Archean-age rock formations, which consist of banded iron formations (BIFs), felsic volcanic, and andesite/diorite lithology (Kwelwa et al., 2018). Certain rocks, particularly BIFs and some volcanic and intrusive rocks, contain NORM such as uraninite and thorite, which harbor uranium, thorium, and their decay products (El Aref et al., 2020). Intermediate rocks like andesite and diorite are also radioactive due to minerals such as amphibole and biotite, which contribute to radiological risks in the mining area (Kwelwa et al., 2018).

2.3. Sampling area

To determine the sampling locations, the AERMOD View Version 21112 dispersion model (Lu et al., 2024), which simulated the spread and concentration of radionuclides based on the local meteorological and environmental conditions (Cimorelli et al., 2004) was used. This version of the AERMOD model was selected due to its advanced capabilities in handling complex dispersion scenarios, including the ability to incorporate detailed local meteorological data and topographical features which are essential for accurate prediction in the mining environment. The AERMOD View Version is widely used in environmental science studies for modelling air quality, ensuring that the simulation results reflect real-world conditions more reliably than other models. The Visual Sampling Plan (VSP) tool was utilized to design a systematic sampling approach, ensuring that the sample collection was statistically representative and unbiased (Bhave & Sadhwani, 2022). This tool was selected for its efficiency in optimizing sampling design, making it suitable for complex environmental assessments and radiological hazard studies (Lolila et al., 2022). The process involved the exportation of annual ground-level concentration isopleths from the AERMOD View program in shape file format to the VSP Tool Version 7.18, following the guidelines provided by the U.S. EPA's Data Quality Objectives (DQO) process. Accordingly, a total of 31 sampling points were systematically plotted and employed for sample collection in the study, as shown in Fig. 2. In addition, judgmental sampling was used to collect five (5) tailings and five (5) waste rock samples at designated locations.

2.4. Sample collection and analysis

A total of thirty-one (31) soil samples were collected at a depth of 0–30 cm using an open-end stainless-steel hand-held Auger corer with a 70 mm diameter from various predetermined locations around the mine, as shown in Fig. 2. Similarly, five (5) tailing samples were collected from a designated location at the tailing storage facility using the same method. Additionally, five (5) waste rock samples were collected using a shovel from designated waste rock dumpsites.

The collected samples were carefully packed and sent to the Tanzania Atomic Energy Commission's laboratory in Arusha for analysis. Upon arrival at the laboratory, the samples were oven-dried at

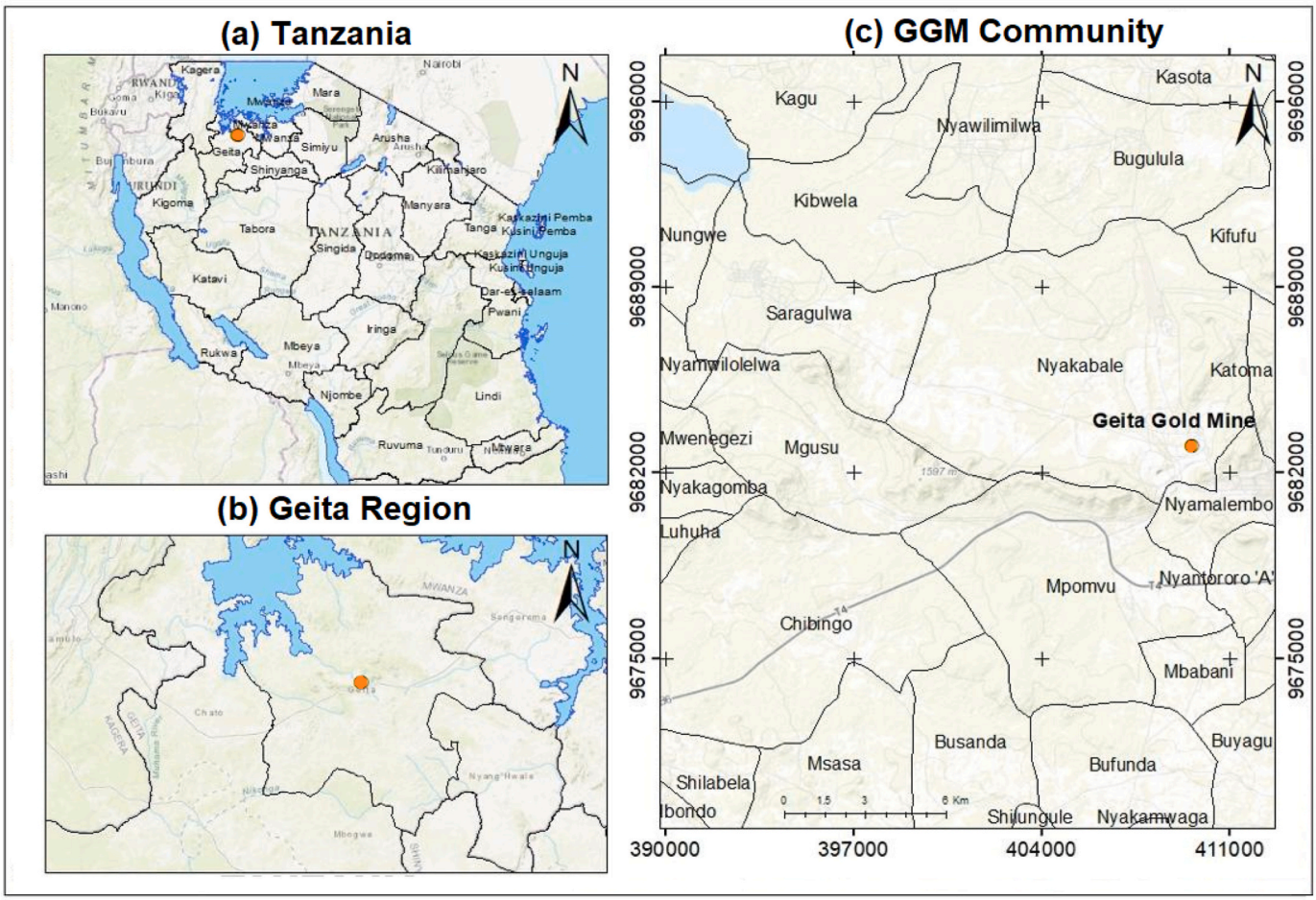

Fig. 1. Shows (a) the location of the Geita Region within Tanzania, (b) the Geita Region, and (c) the villages surrounding the Geita Gold Mine (GGM).

80 °C until they reached a constant weight. The dried samples were then ground and sieved using a 200 μm mesh screen to obtain a fine powder. The sieved samples were then sealed in stainless steel canisters for 4 weeks to allow for the establishment of secular equilibrium between ^{226}Ra, ^{224}Ra, and the short-lived daughters of ^{222}Rn and ^{220}Rn.

2.5. Analysis of radionuclides using gamma spectrometry

The samples' radioactivity concentrations of ^{226}Ra, ^{232}Th, and ^{40}K were measured using a p-type coaxial high-purity germanium detector (ORTEC® GEM40-83-SMP) inside lead shielding and connected to a multichannel analyzer. The detector, with 40 % relative efficiency and specific energy resolutions, was calibrated with a CBSS2 multi-nuclide standard source. The data acquisition and analysis were performed using an ORTEC® DSPEC-LF digital signal processor. The Gamma Vision® software was used in spectrum analysis (ORTEC, 2020). The specific activity concentration of ^{226}Ra in the sample was determined from the gamma-ray peaks at 609.3 keV (from ^{214}Bi) and 351.9 keV (from ^{214}Pb). The concentration of ^{232}Th was measured using the peaks at 583.1 keV (from ^{208}Tl) and 911.2 keV (from ^{228}Ac). The activity concentration of ^{40}K was determined using the 1460.8 keV peak. The activity concentration for each radionuclide of interest was calculated using Eq. (1) (Kovler et al., 2017):

$$A_c = \frac{N_c}{P_\gamma * \varepsilon * T * W} \quad (1)$$

where: A_c stands for the activity concentrations in the samples in Bq kg^{-1}, N_c are the net counts per second (cps), P_γ are the gamma-line emissions probabilities for particular radionuclides, ε are the gamma line emission intensities (%), T are the counting times in seconds (s) of the samples and *W* are the weights in kilogram (kg) of a specific sample.

2.6. Radiological hazard indices

(a) Radium equivalent activity (Ra_{eq})

The radium equivalent activity (Ra_{eq}) is a calculated sum of the hazards associated with ^{226}Ra, ^{232}Th and ^{40}K in a sample. It is crucial for evaluating the overall radiation hazards posed by various radionuclides present in the sample. It was calculated using Eq. (2) (Tufail, 2012):

$$Ra_{eq} = A_{Ra} + 1.43A_{Th} + 0.077A_K \quad (2)$$

where A_{Ra}, A_{Th}, and A_K are the activity concentrations in Bq kg^{-1} of ^{226}Ra, ^{232}Th and ^{40}K, respectively. The accepted safety threshold of Ra_{eq} is 370 Bq kg^{-1} (UNSCEAR, 2020).

(b) External and internal hazard indexes (He_x and H_{in})

The external and internal hazard indices (H_{ex} and H_{in}) were used to assess the hazards imposed by gamma radiation from ^{226}Ra, ^{232}Th, and ^{40}K that are found naturally in soil. The external exposure is caused by direct gamma radiation whereas the internal exposure is due to inhalation of radon and its short-lived decay products. The H_{ex} and H_{in} values were quantified using Eqs. (3) and (4) (Akpanowo et al., 2020):

$$H_{ex} = \frac{A_{Ra}}{370} + \frac{A_{Th}}{259} + \frac{A_K}{4810} \leq 1 \quad (3)$$

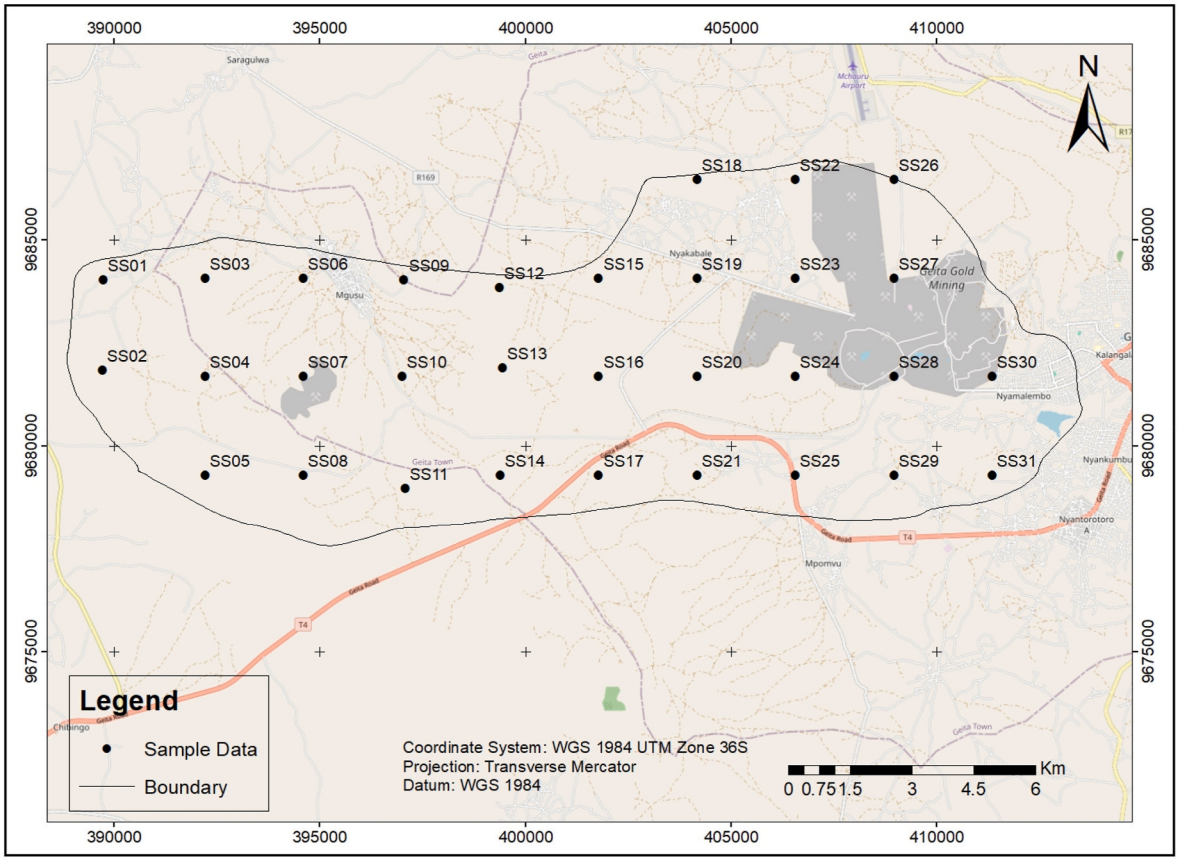

Fig. 2. A map showing the distribution of sampling points with labels.

$$H_{in} = \frac{A_{Ra}}{185} + \frac{A_{Th}}{259} + \frac{A_K}{4810} \leq 1 \quad (4)$$

where A_{Ra}, A_{Th} and A_K assume their respective definitions as earlier stated. The maximum allowed value for H_{ex} and H_{in} is 1, which corresponds to the upper limit of Ra_{eq} (370 Bq kg^{-1}).

(c) Representative gamma index

The representative gamma index (Iγ) is used to evaluate the conformity of soil to dose standards set for building materials (Ayeni & Adebiyi, 2022). The gamma index (Iγ) was computed using Eq. (5) (Darwish et al., 2015; El-Gamal et al., 2007):

$$I_\gamma = \frac{A_{Ra}}{300} + \frac{A_{Th}}{200} + \frac{A_K}{3000} \quad (5)$$

where A_{Ra}, A_{Th} and A_K assume their respective definitions as earlier stated. Radiation safety is considered acceptable if $I_\gamma \leq 1$.

(d) Absorbed gamma dose rate (D_R)

The absorbed gamma dose rate (D_R) at 1 m above the ground surface from the concentration of radionuclides in samples was computed using Eq. (6) (UNSCEAR, 2020)

$$D_R\ (nGyh^{-1}) = 0.462\,A_{Ra} + 0.604A_{Th} + 0.0417A_K \quad (6)$$

where A_{Ra}, A_{Th} and A_K are defined as stated earlier.

(e) Annual effective dose equivalent (AEDE)

The annual effective dose equivalent (AEDE) was calculated using Eq. (7) (Akpanowo et al., 2020; Taskin et al., 2009):

$$AEDE\left(\mu Sv\,y^{-1}\right) = D\left(nGy\,h^{-1}\right)*8760\,h\,y^{-1}*0.2*0.7\left(Sv\,Gy^{-1}\right) \times 10^{-3} \quad (7)$$

An AEDE, limit of 1 mSv y^{-1} is considered acceptable for the general public (UNSCEAR, 2020).

(f) Annual gonadal dose equivalent (AGDE)

The annual gonadal dose equivalent (AGDE) is a measure of the dose received by the gonads (organs responsible for gamete production) of an exposed population over a year (Yachiso et al., 2023). This parameter is important for assessing the potential hereditary effects of radiation exposure to future generations. AGDE was calculated using Eq. (8) (Adebiyi et al., 2021; Yachiso et al., 2023):

$$AGDE\left(\left(\mu Sv\,y^{-1}\right) = 3.09A_{Ra} + 4.18A_{Th} + 0.314A_K \quad (8)$$

where A_{Ra}, A_{Th} and A_K are defined as stated earlier.

(g) Activity utilization index

The activity utilization index (AUI) was calculated from the specific activities of ^{226}Ra, ^{232}Th and ^{40}K in the samples using Eq. (9) (Chandrasekaran et al., 2014):

$$AUI = \left(\frac{A_{Ra}}{50\ Bq\ kg^{-1}}\right)f_{Ra} + \left(\frac{A_{Th}}{50\ Bq\ kg^{-1}}\right)f_{Th} + \left(\frac{A_K}{500\ Bq\ kg^{-1}}\right)f_K \quad (9)$$

where f_{Ra}, f_{Th} and f_K with numerical values of 0.462, 0.604 and 0.041, respectively, represent entire gamma dose fragmentary supplements for ^{226}Ra, ^{232}Th and ^{40}K.

(h) Excess lifetime cancer risk (ELCR)

The excess lifetime cancer risk (ELCR) is a measure of the probability that a certain stochastic effect will occur in an individual exposed to low doses of ionizing radiation over a given period (UNSCEAR, 2020). As such, the ELCR was calculated by using Eq. (10) (Taskin et al., 2009):

$$ELCR = AEDE^{*}DL^{*}F \quad (10)$$

where DL is the average life expectancy (70 years) and RF is the risk factor (0.05 Sv^{-1}) for the general public (UNSCEAR, 2020).

2.7. Statistical and spatial mapping method

IBM SPSS Statistics Version 25 and MS Excel 2016 software for Windows were used for statistical analysis. Whereas the geological and spatial maps were created using QGIS Version 3.16. In addition, the Kriging interpolation technique, a geostatistical method, was applied to create spatial distribution maps for radionuclide concentrations and radiological indices. This method provided a reliable estimation of values in unmeasured locations by considering both the distance and the degree of variation between measured data points, enhancing the accuracy of spatial analysis.

3. Results and discussion

3.1. Activity concentrations of ^{226}Ra, ^{232}Th, and ^{40}K for soil at GGM

The activity concentrations of ^{226}Ra, ^{232}Th, and ^{40}K in soil samples collected from various locations surrounding the GGM are shown in Table 1. The activity concentration of ^{226}Ra ranged from 13 ± 9 to 99 ± 4 Bq kg^{-1}, with an average of 54 ± 3 Bq kg^{-1}. The activity of concentration of ^{232}Th ranged from 12 ± 10 to 74 ± 2 Bq kg^{-1}, with an average of 45 ± 1 Bq kg^{-1}. For ^{40}K the activity concentration ranged from 70 ± 6 to 745 ± 2 Bq kg^{-1}, with an average of 279 ± 1 Bq kg^{-1}. Compared to the global average values reported by UNSCEAR, 2020 of 35 Bq kg^{-1} for ^{226}Ra, 45 Bq kg^{-1} for ^{232}Th and 420 Bq kg^{-1} for ^{40}K, the average activity concentration of ^{232}Th and ^{40}K in this study area are lower. The elevated levels of ^{226}Ra exceed the global average values (UNSCEAR, 2020). The elevated levels of ^{226}Ra may be attributed to variations in physical and chemical properties of the soil along with solubility of radionuclides in similar environmental condition (Pappa et al., 2016).

The elevated activity concentration of ^{226}Ra could also be associated with the geological characteristics of the study area, which is composed of intrusive rocks like andesite and diorite (Kileo et al., 2025). These rocks are known to contain minerals such as amphibole and biotite, and uranium-bearing minerals that contribute to higher ^{226}Ra levels (Kwelwa et al., 2018; Saleh et al., 2021). Additionally, land reclamation processes at the mine often involve waste rocks derived from excavation activities, which may further increase the 226Ra activity concentration due to uranium-bearing rocks. Notably, most sampling points situated in the Nyakanga underground mine recorded activity concentrations that exceeded the global averages of 32 Bq kg^{-1} and 45 Bq kg^{-1} for ^{226}Ra and ^{232}Th, respectively. This trend reflects the influence of mining activities and geological formations such as BIFs, which are rich in NORM (Kwelwa et al., 2018).

Table 2 provides a comparative summary of activity concentration obtained in this study and those reported in literature from other gold mining regions across Africa, as well a global reference values. The average ^{226}Ra concentration of 54 Bq kg^{-1} in this study exceeds the global average but is lower than the values found at other locations.

The average activity concentration value of ^{226}Ra in this study (54 Bq kg^{-1}) exceeds the global average value but is still lower than 60 Bq kg^{-1} that was for instance reported in Ghana (Faanu et al., 2012), 60 and 62 Bq kg^{-1} reported in Nigeria by Amodu et al. (2024) and Odelami et al. (2024) (See Table 2). Meanwhile, except for the values in Chad that were reported by Samafou et al. (2023), studies from other regions (Faanu et al., 2012; Odelami et al., 2024; Reddy et al., 2017; Yachiso et al., 2023) report elevated activity concentrations for ^{232}Th and ^{40}K.

These discrepancies in concentrations across various studies suggest that local geological settings and mining activities may significantly influence the radionuclide content in soils. While the results from this study indicate a moderate enhancement of ^{226}Ra above the global average, elevated concentration in other mining sites reflect diverse geological and operational contexts. This observation underscores the importance of conducting localized radiological assessments rather than relying solely on global averages.

3.2. Radiological hazard indices of soil samples around the GGM

Table 3 presents a summary of the statistical results for the radiological hazard indices of soil around the GGM site using different activity indices calculated from the activity concentrations of ^{226}Ra, ^{232}Th, and ^{40}K measured in soil samples collected around the mine area.

The Ra_{eq} varied from 50 ± 4 to 227 ± 5 Bq kg^{-1} with an average of 139 ± 5 Bq kg^{-1}, indicating a considerable variability across the samples. Despite this variability, the results showed that the obtained Ra_{eq} values were below the acceptable value of 370 Bq kg^{-1}, which corresponds to an annual dose of 1 mSv y^{-1} to members of the public as reported by UNSCEAR, 2020. As such, the Ra_{eq} value in soil samples from the study area could be within safe limits, thus minimizing concerns about potential exposure to harmful radiation levels in the studied area.

Table 3 also presents the external (H_{ex}) and internal (H_{in}) hazard indices for the analyzed soil samples. The H_{ex} ranged from 0.08 ± 0.01 to 0.62 ± 0.02 Bq kg^{-1} with an average of 0.35 ± 0.5 Bq kg^{-1}, while the H_{in} ranged from 0.17 ± 0.02 to 0.86 ± 0.02 with an average of 0.53 ±

Table 2
Comparative analysis of activity concentration of soil (Bq kg^{-1}) around the Geita Gold Mine (GGM) with other mines, including global average values.

Country	Activity concentration (Bq kg^{-1})			References
	$^{238}U/^{226}Ra$	^{232}Th	^{40}K	
Tanzania	54 ± 3	45 ± 2	279 ± 1	This study
Ethiopia	4	53	392	Yachiso et al. (2023)
Chad	30	12	234	Samafou et al. (2023)
Ghana	64	68	1244	Faanu et al. (2012)
India	27	63	818	Reddy et al. (2017)
Nigeria	60	161	665	Odelami et al. (2024)
Nigeria	62	73	1135	Amodu et al. (2024)
Global mean value	35	45	420	UNSCEAR, 2020

Table 1
Comparison of the activity concentration of ^{226}Ra, ^{232}Th, and ^{40}K of soil with the global average values.

	Range (Bq kg^{-1})	Min. (Bq kg^{-1})	Max. (Bq kg^{-1})	Mean ± SD[a] (Bq kg^{-1})	Global mean (UNSCEAR, 2020) (Bq kg^{-1})
^{226}Ra	86	13 ± 9	99 ± 4	54 ± 3	35
^{232}Th	62	12 ± 10	74 ± 2	45 ± 2	45
^{40}K	675	70 ± 6	745 ± 2	279 ± 1	420

Table 3
Comparative analysis of radiological indices of soil around Geita Gold Mine (GGM) with global average values.

	Range	Minimum	Maximum	Mean ± SD[a]	Global mean (UNSCEAR, 2020)
Radiation indices					
Ra_{eq} (Bq kg^{-1})	178	50	227	139 ± 5	370
H_{ex}	0.54	0.08	0.62	0.35 ± 0.50	≤1
H_{in}	0.69	0.17	0.86	0.53 ± 0.01	≤1
D_R (nGy h^{-1})	97	24	121	69 ± 1.85	59
AEDE (nGy h^{-1})	100	30	130	78 ± 3	70
AGDE (mSv)	573	172	745	430 ± 13	300
AUI	1.46	0.30	1.76	1 ± 0.30	≤2
Gamma (I_γ)	0.64	0.19	0.83	0.49 ± 0.01	≤1
$ELCR_{out}$ × 10^{-3}	0.36	0.1	0.46	0.27 ± 0.10	0.29

0.01 It is noteworthy that all the obtained H_{ex} and H_{in} values reported in this work were below the value of 1, thus minimizing the potential external and internal hazards due to harmful radiation in the studied areas especially when the soil from a certain area is going to be used as a building material. The average H_{ex} value in this study area is lower than values reported in other countries, such as 0.61 in Kano, Nigeria (Bello, Nasiru, Garba, & Adeyemo, 2019), 2.4 in Gauteng South Africa (Kamunda et al., 2016) and 0.84 in China (Zhang, Huang, Yang, Tu, & Jin, 2020). Similarly, the average H_{in} value of the current study is lower if compared to the 0.70 reported for the Rosterman Gold Mine in Kenya (Khisa Wanyama et al., 2020).

The representative gamma index (I_γ) values ranged from 0.19 ± 0.02 to 0.83 ± 0.02 with an average of 0.49 ± 0.01, as shown in Table 3. This value was 51 % lower than the recommended threshold of 1, as stipulated by UNSCEAR, 2020. Additionally, the activity utilization index (AUI) ranged from 0.50 ± 0.09 to 1.83 ± 0.07 with an average of 0.98 ± 0.07. Although the average AUI value was approximately equal to 1, it remains below the recommended threshold of 2, which corresponds to an annual effective dose of less than 0.3 mSv y^{-1} (UNSCEAR, 2020). Similar studies, conducted in Gauteng, South Africa (Kamunda et al., 2016), and Nigeria (Osimobi, Avwiri, & Agbalagba, 2018), reported higher values exceeding the average representative gamma index (I_γ) and AUI values obtained in this study, indicating potential radiological risks. In contrast, the current study remains well below the threshold, suggesting a comparatively safer condition. These findings indicate that radiation exposure levels in the study area are within acceptable public health limits and suggest that the soil is safe for unrestricted use in construction without posing significant radiological risks. It is important to note that these indices do not account for the potential concentration of NORM through weathering or processing.

3.2.1. *Absorbed dose rate (D_R) and annual effective dose equivalent (AEDE)*

The gamma absorbed dose rate D_R ranged from 24 ± 2 to 121 ± 2 nGy h^{-1}, averaging 68 ± 2 nGy h^{-1}, while the annual effective dose equivalent (AEDE) ranged from 30 ± 2 to 130 ± 3 μSv y^{-1}, with an average of 78 ± 25 μSv y^{-1} (Table 3). Both the average D_R and AEDE values were slightly above the global averages of 59 nGy h^{-1} and 70 μSv y^{-1}, respectively, as reported by UNSCEAR, 2020. This elevation may be attributed to geological factors such as the mineral composition of the soils or the presence of specific rock types in the study area (Kileo et al., 2025). Nonetheless, the AEDE remains below the recommended limit of 1 mSv y^{-1} for the public as stipulated by UNSCEAR, 2020 and ICRP (2019). Although the radiation levels are elevated compared to worldwide background levels, they do not pose an immediate health risk under current international guidelines. However, it is important to consider that chronic exposure, even at lower levels, could result in cumulative effects over time, especially for populations residing near areas with ongoing mining activities. As such, future studies could investigate the sources of variability in radionuclide concentrations and explore potential correlations with other environmental parameters, such as soil type, land use, and weathering processes.

3.2.2. *Annual gonadal equivalent dose (AGED) and excess life cancer rate (ELCR)*

The annual gonadal dose equivalent (AGDE) values computed in this work ranged from 172 ± 13 to 745 ± 17 μSv y^{-1}, with an average of 430 ± 13 μSv y^{-1}, exceeding the global average value of 300 μSv y^{-1} by approximately 42 %. While this indicates a higher radiation burden on sensitive reproductive tissues, it is still slightly lower than AGDE values reported in other African mining regions, where values were reported to be as high as 439.73 μSv y^{-1} (Ademola, Bello, & Adejumobi, 2014) for Ghana and even 2083 μSv y^{-1} (Aborisade et al., 2018) for Nigeria. Additionally, the AGDE in this study is comparable to findings in southeastern Nigeria, where the average value were reported to be around 414 μSv (Tunde Ogundele et al., 2021). The relatively high AGDE values observed in this study are likely influenced by the elevated concentrations of ^{226}Ra and ^{232}Th, which contribute significantly to gonadal radiation exposure. Although the average AGDE indicates somewhat higher radiation exposure than the global average for soil, it remains below the threshold of 1 mS y^{-1} for significant radiological health hazards.

The excess life cancer risk (ELCR) quantifies the probability of developing cancer over a lifetime at a given exposure rate (Atipo et al., 2020). In this study, the average ELCR ranged from 0.10 × 10^{-3} to 0.46 × 10^{-3} with an average of (0.27 ± 0.01) × 10^{-3}. These findings indicate that the ELCR from external exposure in the study area can be considered low. Importantly, the observed ELCR was below the global threshold of 0.29 × 10^{-3} as specified by UNSCEAR, 2020, suggesting that, under current conditions, the radiological exposure from the measured radionuclides poses a minimal radiological health risk to the local population. Nevertheless, it is important to consider that environmental conditions and exposure scenarios may change over time. As such, ongoing monitoring is essential, particularly in regions impacted by mining activities, to detect any shifts in radionuclide concentrations or exposure pathways.

3.3. *Activity concentrations of ^{226}Ra, ^{232}Th, and ^{40}K in tailings*

The activity concentrations of ^{226}Ra, ^{232}Th, and ^{40}K in tailings ranged from 66 ± 1.2 to 73 ± 3 Bq kg^{-1} with an average activity concentration of 70 ± 2 Bq kg^{-1} for ^{226}Ra, while that of ^{232}Th ranged from 32 ± 1.5 to 39 ± 1.6 Bq kg^{-1} with an average activity concentration of 36 ± 2 Bq kg^{-1}. For ^{40}K the activity concentration ranged from 820 ± 74 to 964 ± 89 Bq kg^{-1} with an average activity concentration of 878 ± 80 Bq kg^{-1} as shown in Table 4. The activity concentrations of ^{226}Ra and

Table 4
Comparison of the activity concentration of ^{226}Ra, ^{232}Th, and ^{40}K of tailings with the global average values.

Sample ID	Specific Activity Concentration (Bq kg^{-1})		
	^{226}Ra	^{232} Th	^{40}K
TS1	72	36	881
TS2	66	32	820
TS3	73	36	964
TS4	69	38	858
TS5	69	39	867
Range	66–73	32–39	820–964
Average ± SD[a]	70 ± 2	36 ± 2	878 ± 80
Global mean values (UNSCEAR, 2020)	35	45	420

Table 5
Comparative analysis of activity concentration of tailings (Bq kg^{-1}) around Geita Gold Mine (GGM) with other mines, including global average values.

Country	Activity concentration (Bq kg^{-1})			References
	^{226}Ra	^{232}Th	^{40}K	
Tanzania	70	36	878	This study
South Africa	485.3	43.9	422.6	Kamunda et al. (2016)
Uganda	58.7	193.5	892.9	Silver et al. (2016)
Nigeria	14.5	10.45	332.7	Bamidele and Edun (2024)
Fiji	19.5	129.06	86	Rabuku and Malik (2020)
Global mean	35	45	420	UNSCEAR, 2020

^{40}K in the tailings were approximately twice the global average values of 35 Bq kg^{-1} and 420 Bq kg^{-1}, respectively (UNSCEAR, 2020). These elevated levels suggest a significant accumulation of radionuclides in the waste materials generated during gold extraction. Comparable studies conducted in South Africa and Uganda have also reported elevated radionuclide concentrations in gold mine tailings, further emphasizing the need for stringent monitoring and mitigation strategies (Kamunda et al., 2016; Silvester, Lowndes, & Hargreaves, 2009). Such accumulations pose potential environmental and public health risks, especially when tailings are inadequately managed or used in construction or agriculture.

The exceedance of the activity concentration of ^{40}K could be attributed to the geological characteristics of the Archean green belt geology, with gold mineralization hosted in mafic volcanic rocks and sedimentary units with shear zones and faults (Kileo et al., 2025; Kwelwa et al., 2018). To further contextualize the data, the summarized findings were compared with other literature data from different gold mines in Table 5. Radiological hazard indices of the tailings were further compared to global averages in Table 6.

While the average activity concentration of ^{226}Ra, ^{232}Th, and ^{40}K in this study exceeded the global average values reported by UNSCEAR, 2020, they also surpassed the value of 14.5 Bq kg^{-1}, 10.45 Bq kg^{-1} and 332.7 Bq kg^{-1} reported by Bamidele and Edun (2024) for a gold mine in Nigeria. In contrast, the activity concentration values of ^{232}Th, and ^{40}K reported in this study were lower than 193 Bq kg^{-1} and 892.9 Bq kg^{-1} as reported by Silver et al. (2016) for tailings of the Mashonga gold mine in Uganda. Furthermore, the activity concentration of ^{226}Ra in the current study is approximately 86 % lower than the 485 Bq kg^{-1} reported by Kamunda et al. (2016) for tailings at a gold mine in Gauteng, South Africa. These differences reflect the variations in radionuclide concentrations that are influenced by geological formation. Geological formations such as BIFs, felsic volcanic rocks, and intrusive rocks like andesite and diorite, common in the Geita region, are often enriched with uranium and thorium-bearing minerals so that they can show elevated NORM concentrations (Kileo et al., 2025).

Table 8
Calculated activity concentrations of radionuclides in waste rocks, compared to global average values.

Sample ID	Specific Activity Concentration (Bq kg^{-1})		
	^{226}Ra	^{232}Th	^{40}K
WR1	70 ± 2.3	49 ± 1.6	672 ± 13
WR2	73 ± 2.9	95 ± 2.1	707 ± 14
WR3	62 ± 1.8	77 ± 1.1	729 ± 19
WR4	59 ± 1.6	66 ± 1.9	628 ± 16
WR5	69 ± 2.1	79 ± 2.7	567 ± 14
Range	59 ± 1.6–73 ± 3	49 ± 2–95 ± 2	567 ± 14–729 ± 19
Average ± SD[a]	67 ± 1	73 ± 1	661 ± 7
Global mean (UNSCEAR, 2020)	35	45	420

3.4. Radiological hazard indices (Ra_{eq}, H_{in}, H_{ex}, I_γ and AUI) of tailings

Table 7 shows the summary of calculated radiological hazard indices of the analyzed tailings. The Ra_{eq} values ranged from 176 ± 7 to 199 ± Bq kg^{-1} with an average of 189 ± 8 Bq kg$^{-1,}$ showing moderate variability across the samples. The obtained average Ra_{eq} value in the tailing samples was found to be approximately 49 % lower than the Ra_{eq} value of 370 Bq kg^{-1}, which corresponds to an annual effective dose of 1 mSv y^{-1} (UNSCEAR, 2020) (see Table 8).

Furthermore, the average Ra_{eq} value obtained in the study area was approximately 57 % lower than the Ra_{eq} value of 439.2 Bq kg^{-1} reported by Silver et al. (2016) for tailings at the Mashonga gold Mine in Uganda. This difference could likely be attributed to variations in the local geology and mining practices, since the Mashonga mine site may have more uranium-rich deposits or more intensive mining operations that could liberate more radionuclides.

The calculated average H_{ex} values from the mine tailings ranged from 0.47 ± 0.02 to 0.54 ± 0.02, with an overall average of 0.51 ± 0.02.

Table 6
Radiological hazard indices (Ra_{eq}, H_{ex}, H_{in}, I_γ, and AUI) of tailings, compared to global average values.

Sample ID	Ra_{eq} (Bq kg^{-1})	H_{ex}	H_{in}	I_γ	AUI
TS1	191	0.52	0.71	0.71	1.17
TS2	176	0.47	0.65	0.66	1.07
TS3	199	0.54	0.73	0.74	1.19
TS4	188	0.51	0.69	0.70	1.16
TS5	192	0.52	0.70	0.71	1.18
Range	176–199	0.47–0.54	0.65–0.73	0.66–0.71	1.07–1.19
Average ± SD[a]	189 ± 8	0.51 ± 0.02	0.69 ± 0.02	0.71 ± 0.02	1.15 ± 0.03
Global mean (UNSCEAR, 2020)	370	≤1	≤1	≤1	≤2

Table 7
Radiological hazard indices (D_R, AEDE, AGDE, and ELCR) of tailings, compared to global average values.

Sample ID	D_R (nGy h^{-1})	AEDE (μSv y^{-1})	AGDE (μSv)	ELCR × 10^{-3}
TS1	92	112	597	0.36
TS2	84	103	678	0.34
TS3	96	117	638	0.38
TS4	90	111	648	0.36
TS5	92	112	377	0.37
Range	84–96	103–117	597–678	0.36–0.41
Average ± SD[a]	91 ± 4	111 ± 6	642 ± 12	0.39 ± 0.003
Global mean (UNSCEAR, 2020)	59	70	≤1000	0.29

Similarly, the H_{in} values ranged from 0.65 ± 0.02 to 0.73 ± 0.03, with an average value of 0.70 ± 0.02 (Table 7). These averages are approximately 49 % and 30 % lower than the threshold value of 1, as recommended by UNSCEAR, 2020, indicating that the radiological hazards from the tailings are within acceptable safety limits for public exposure.

When compared with findings from other mining regions, the hazard indices in the present study are comparatively low. For example, Kamunda et al. (2016) reported significantly elevated H_{ex} and H_{in} values at 2.4 and 4.5, respectively, in gold mining areas of Gauteng, South Africa. Similarly, Olayemi et al. (2024) observed hazard indices of 2.39 and 4.15 in pegmatite mines at Komu in southwestern Nigeria, implying substantially higher risks in those regions compared to the tailings of the GGM.

The lower hazard indices in the present study can be attributed to moderate activity concentrations of radionuclides, particularly ^{226}Ra and ^{232}Th, in the tailings. This suggests that although mining processes at the GGM lead to a redistribution of NORM, the degree of enrichment is less severe than in other regions with similar activities. Nevertheless, continuous monitoring is essential to ensure that future changes in radionuclide leaching or environmental conditions are promptly identified, particularly in areas near residential or agricultural zones that are adjacent to the tailings storage facility.

The calculated gamma index (Iγ) values for tailings ranged from 0.66 ± 0.03 to 0.71 ± 0.03, with an average of 0.71 ± 0.03. This value is below the threshold limit of 1, as recommended by (UNSCEAR, 2020).

The calculated activity utilization index (AUI) values for tailings ranged from 1.07 ± 0.16 to 1.19 ± 0.19, with an average of 1.15 ± 0.017. This average AUI value is below the safety threshold of 2, which corresponds to an annual effective dose of less than 0.3 mSv y^{-1} (El-Gamal et al., 2007). These findings indicate that the tailings at the GGM site may exhibit relatively low radionuclide enrichment in terms of their contribution to radiological exposure. An AUI value below the threshold suggests that the tailings do not contribute significantly to the external dose, thereby reducing the likelihood of adverse health effects in the surrounding population.

3.5. Radiological hazard indices (D_R, AEDE, AGDE and ELCR) of tailings

The average D_R values for tailings ranged from 84 ± 4 to 96 ± 4 nGy h^{-1}, with a mean of 91 ± 4 nGy h^{-1} (See Table 7). The mean D_R value is approximately 35 % higher than the global outdoor mean value of D_R of 59 nGy h^{-1} reported by UNSCEAR, 2020. The elevated D_R in tailings indicates a slightly enhanced concentration of radionuclides, particularly ^{226}Ra and ^{232}Th, which can be directly linked to the geological characteristics of the mined ore and the methods used for mineral extraction and processing. Compared to other regional studies, the D_R value in this study was about 78 % lower than the values of 407 and 413.5 nGy h^{-1} reported for tailings in South Africa by Moshupya et al. (2022) and Kamunda et al. (2016), respectively. Furthermore, the average D_R value is about 50 % lower than the 191.2 nGy h^{-1} reported for tailings at the Mashonga Gold Mine in Uganda (Silver et al., 2016). The disparities in these dose rates likely reflect differences in the geological formation of the respective mine sites as well as differences in the processing methods. The observed D_R value at the GGM is unlikely to cause adverse radiological effects. However, localized variations and prolonged exposures warrant further investigation to fully ascertain any long-term radiological implications.

On the other hand, the calculated AEDE values from tailings ranged from 103 ± 6 to 117 ± 6 μSv y^{-1}, with an average of 111 ± 2 μSv y^{-1}. This average value was approximately 37 % higher than the global average AEDE value of 70 μSv y^{-1} for outdoor terrestrial radiation, as reported by UNSCEAR, 2020. The elevated AEDE value can primarily be attributed to the increased absorbed dose rate (D_R) observed in the tailings. Since the AEDE is derived from the D_R, the enhanced presence of natural radionuclides, particularly ^{226}Ra and ^{232}Th, directly contributes to the higher effective dose received by individuals living or working in the proximity to the mine. When compared with findings from other mines, the observed AEDE values in this study aligned with the results reported by Kamunda et al. (2016), who found slightly higher AEDE values of 120 μSv y^{-1} in South African mine tailings, likely due to elevated concentrations of thorium and radium. Similarly, the present AEDE is significantly lower (71 % lower) than the higher value of 390 μSv y^{-1} reported by Silver et al. (2016) for the Mashonga Gold Mine in Uganda. While the AEDE values in this study remain below the recommended public exposure limit of 1000 μSv y^{-1} ICRP (2007), the cumulative exposure over time, particularly for workers and local populations still warrants continuous monitoring.

The AGDE values for the tailings ranged from 597 ± 27 to 678 ± 27 μSv y^{-1}, with an average of 678 ± 12 μSv y^{-1}. This average AGDE value exceeds the global average of 300 μSv y^{-1} reported by UNSCEAR, 2020 by approximately 53 %, indicating an increased radiological burden on the gonadal tissues of individuals exposed to the tailings. The elevated AGDE values could be attributed to the enhanced concentrations of radionuclides, particularly ^{226}Ra, ^{232}Th, and ^{40}K, present in the tailings. Given that gonadal tissues are among the most radiosensitive organs (UNSCEAR, 2020), prolonged exposure even at these levels could increase the risks of heritable genetic mutation and reproducibility health effects. Comparative studies in other mining environments also report elevated AGDE values. For example, Aborisade et al. (2018) reported values exceeding 2000 μSv y^{-1} in Nigerian gold mining sites, while Tunde Ogundele et al. (2021) observed average values around 414 μSv y^{-1} in southeastern Nigeria. Although the AGDE values at the GGM site are lower than some high-risk sites, the present levels still warrant caution and continued monitoring, especially in communities near tailings storage facilities or where tailings are repurposed for agriculture or construction.

The estimated ELCR values for the tailings ranged from (0.36 ± 0.02) × 10^{-3} to (0.41 ± 0.02) × 10^{-3} with an average of (0.39 ± 0.004) × 10^{-3}. This average exceeds the global average threshold of 0.29 × 10^{-3} reported by UNSCEAR, 2020, representing an approximate 20 % increase above the global average. However, the ELCR values observed in this study are significantly lower by 74 % than the value of 1.3 × 10^{-3} reported by Silver et al. (2016) for tailings from the Mashonga gold mine in Uganda. These comparative results suggest that while the ELCR in the present study is elevated relative to the global average, it is still significantly lower than values observed in other gold mining regions.

Table 9
Radiological hazard indices (Ra_{eq}, H_{ex}, H_{in}, I_γ, and AUI) of waste rocks, compared to global average values.

Sample ID	Ra_{eq} (Bq kg^{-1})	H_{ex}	H_{in}	Iγ	AUI
WR1	193 ± 3	0.52 ± 0.01	0.71 ± 0.01	0.71 ± 0.01	1.30 ± 0.1
WR2	264 ± 4	0.71 ± 0.01	0.91 ± 0.02	0.96 ± 0.02	1.89 ± 0.1
WR3	120 ± 3	0.32 ± 0.01	0.49 ± 0.01	0.41 ± 0.01	1.04 ± 0.1
WR4	200 ± 3	0.54 ± 0.01	0.70 ± 0.01	0.73 ± 0.01	1.38 ± 0.1
WR5	226 ± 5	0.61 ± 0.01	0.80 ± 0.02	0.81 ± 0.02	1.64 ± 0.1
Range	193–226	0.32–0.71	0.49–0.91	0.41–0.96	1.04–1.89
Average ± SD[a]	200 ± 2	0.54 ± 0.01	0.72 ± 0.04	0.72 ± 0.01	1.45 ± 0.03
Global mean (UNSCEAR, 2020)	370	≤1	≤1	≤1	≤2

Table 10
Radiological hazard indices (D_R, AEDE, AGDE and ELCR) of waste rocks, compared to global average values.

Sample ID	D_R (nGy h^{-1})	AEDE (μSv h^{-1})	AGDE (μSv)	ELCR × 10^{-3}
WR1	71 ± 2	87 ± 11	648 ± 6	0.31 ± 0.02
WR2	121 ± 2	149 ± 13	597 ± 6	0.52 ± 0.02
WR3	53 ± 1	65 ± 9	698 ± 5	0.23 ± 0.02
WR4	93 ± 2	114 ± 10	638 ± 3	0.40 ± 0.02
WR5	103 ± 2	127 ± 14	648 ± 6	0.44 ± 0.02
Range	53–121	65–149	597–698	0.23–0.52
Average ± SD[a]	88 ± 1	108 ± 5	642 ± 2	0.38 ± 0.01
Global mean (UNSCEAR, 2020)	59	70	300	0.29

However, there are concerns regarding potential health risks associated with the use of these tailings for construction purposes, as the estimated radiological parameters exceed the recommended safety limits.

3.6. Activity concentrations of ^{226}Ra, ^{232}Th, and ^{40}K in waste rocks

The activity concentrations of ^{226}Ra, ^{232}Th, and ^{40}K in waste rocks ranged from 59 ± 1.6 to 73 ± 3 Bq kg^{-1} with an average activity concentration of 67 ± 1 Bq kg^{-1} for ^{226}Ra, while that of ^{232}Th ranged from 49 ± 2 to 95 ± 2 Bq kg^{-1} with an average activity concentration of 73 ± 1 Bq kg^{-1}. For ^{40}K, the activity concentration ranged from 567 ± 14 to 729 ± 19 Bq kg^{-1} with an average activity concentration of 661 ± 7 Bq kg^{-1} for ^{40}K as shown in Table 9. The obtained activity concentration values of ^{226}Ra, ^{232}Th, and ^{40}K are 47 %, 38 % and 36 % higher than the global average values of 35 Bq kg^{-1} for ^{226}Ra, 45 Bq kg^{-1} for ^{232}Th, and 420 Bq kg^{-1} for ^{40}K, respectively as reported by UNSCEAR, 2020 (Table 10). These elevated activity concentrations suggest that the waste rocks contain higher levels of NORM compared to the global averages, which may pose radiological concerns if the waste rocks are not properly managed. The higher concentration of ^{226}Ra in particular is noteworthy, as radium isotopes are known to be more radiotoxic and can pose long-term health risks. The presence of ^{40}K at relatively high levels, while not as radiotoxic as radium or thorium, can still contribute to overall radiological exposure, particularly when the waste rocks are close to human habitation or utilized as construction materials.

The high activity concentration of ^{226}Ra, ^{232}Th and ^{40}K in the waste rocks could be attributed to the presence of intrusive igneous rocks, which are linked to the BIFs, which are known to have uranium and thorium (Kileo et al., 2025).

3.7. Radiological hazard indices (Ra_{eq}, H_{in}, H_{ex}, I_γ and AUI) of waste rocks

The Ra_{eq} values in waste rocks ranged from 120 ± 3 to 264 ± 4 Bq kg^{-1}, with an average of 200 ± 2 Bq kg^{-1} (See Table 9). The measured average Ra_{eq} value is 46 % lower than the global threshold of 370 Bq kg^{-1}, which corresponds to an annual effective dose of 1 mSv y^{-1} for members of the public. Since the average Ra_{eq} in this study is significantly below the threshold value, it suggests that the radiological hazard from these waste rocks is likely to be minimal under typical exposure scenarios.

The calculated H_{ex} and H_{in} values ranged from 0.32 ± 0.01 to 0.71 ± 0.01 and 0.49 ± 0.01 to 0.96 ± 0.02 with average values of 0.72 ± 0.04 for H_{ex} and 0.54 ± 0.01 for H_{in}. Both indices are below the safety threshold of 1 recommended by UNSCEAR, 2020, indicating minimal radiological health risks to the local population from the waste rocks. Compared to similar studies, Silver et al. (2016) reported average H_{ex} and H_{in} values of 1.1 and 1.3 at the Mashonga gold mine in Uganda.

The gamma index (I_γ) ranged from 0.41 ± 0.01 to 0.96 ± 0.02 with an average of 0.72 ± 0.01. The average value of I_γ did not exceed the threshold value of 1 reported by UNSCEAR, 2020, indicating that the radiological risks associated with the measured waste rocks are within acceptable limits. However, the potential long-term exposure risks suggest that the waste rocks may not be entirely safe for use as construction materials. It is noteworthy that other studies reported higher I_γ values. At the Mashonga mine in Southwestern Uganda, Silver et al. (2016) reported for instance an average I_γ value of 1.5, which is 33 % higher than the value in this study. These comparisons highlight how important the local geology is for determining the gamma indices. Areas rich in uranium-containing minerals often show higher gamma index values. Studies done in uranium-rich mining locations in South Africa (Kamunda et al., 2016) for example, have shown higher gamma index values, which closely correspond with the presence of uranium-bearing materials. Comparably, studies conducted in gold mining areas in Ghana (Faanu et al., 2016) show that greater gamma index values are correlated with heightened radioactive concentrations. These results are in line with international studies (UNSCEAR, 2019) stressing how the ambient radiological dangers depend on the mineralogical makeup of a given location.

The activity utilization index (AUI) obtained for the waste rocks ranged from 1.04 ± 0.01 to 1.89 ± 0.1 with an average value of 1.45 ± 0.03. These values are below the threshold of 2, corresponding to an AEDE value below 1 mSv y^{-1}

3.8. Radiological hazard indices (D_R, AEDE, AGDE and ELCR) of waste rocks

The gamma absorbed dose rate (D_R) from the investigated waste rocks ranged from 53 ± 1 to 121 ± 2 nGy h^{-1}, with an average value of 88 ± 1 nGy h^{-1}. This average D_R is about 32 % higher than the worldwide average value of 59 nGy h^{-1} reported by UNSCEAR, 2020. Compared to similar studies, the D_R is about half as low as the value of 181.2 nGy h^{-1} reported by Silver et al. (2016) at the Mashonga gold mine in Uganda.

Despite the higher values compared to the global average, the D_R in this study is still within the range observed in other mining environments, suggesting manageable radiological risks. However, the AEDE from the waste rocks ranged from 65 ± 13 to 149 ± 13 μSv y^{-1} with an average of 108 ± 5 μSv y^{-1}. The average AEDE value was approximately 35 % higher than the global average of 70 μSv y^{-1} reported by UNSCEAR, 2020. In comparison with other studies, the AEDE in this study is 70 % lower than the reported AEDE of 370 μSv y^{-1}, at the Mashonga gold mine Silver et al. (2016) and about 14 % higher than the value of 93 μSv y^{-1} recorded at the Perseus Mine in Ghana (Faanu et al., 2016).

The AGDE ranged from 597 ± 6 to 648 ± 6 μSv y^{-1} with an average of 642 ± 2 μSv y^{-1}. This value is approximately 2 times higher than the global average value of 300 μS y^{-1} as reported by UNSCEAR, 2020, which indicates significant radiological risks to sensitive tissues, particularly the reproductive organs, from prolonged exposure. The close similarity suggests comparable radionuclide distributions and geochemical compositions in the waste rocks of both study areas. The elevated AGDE levels are likely attributed to thorium-rich minerals in the study area.

The estimated early lifetime cancer risk (ELCR) values obtained from the waste rocks ranged from (0.23 ± 0.02) × 10^{-3} to (0.52 ± 0.02) ×

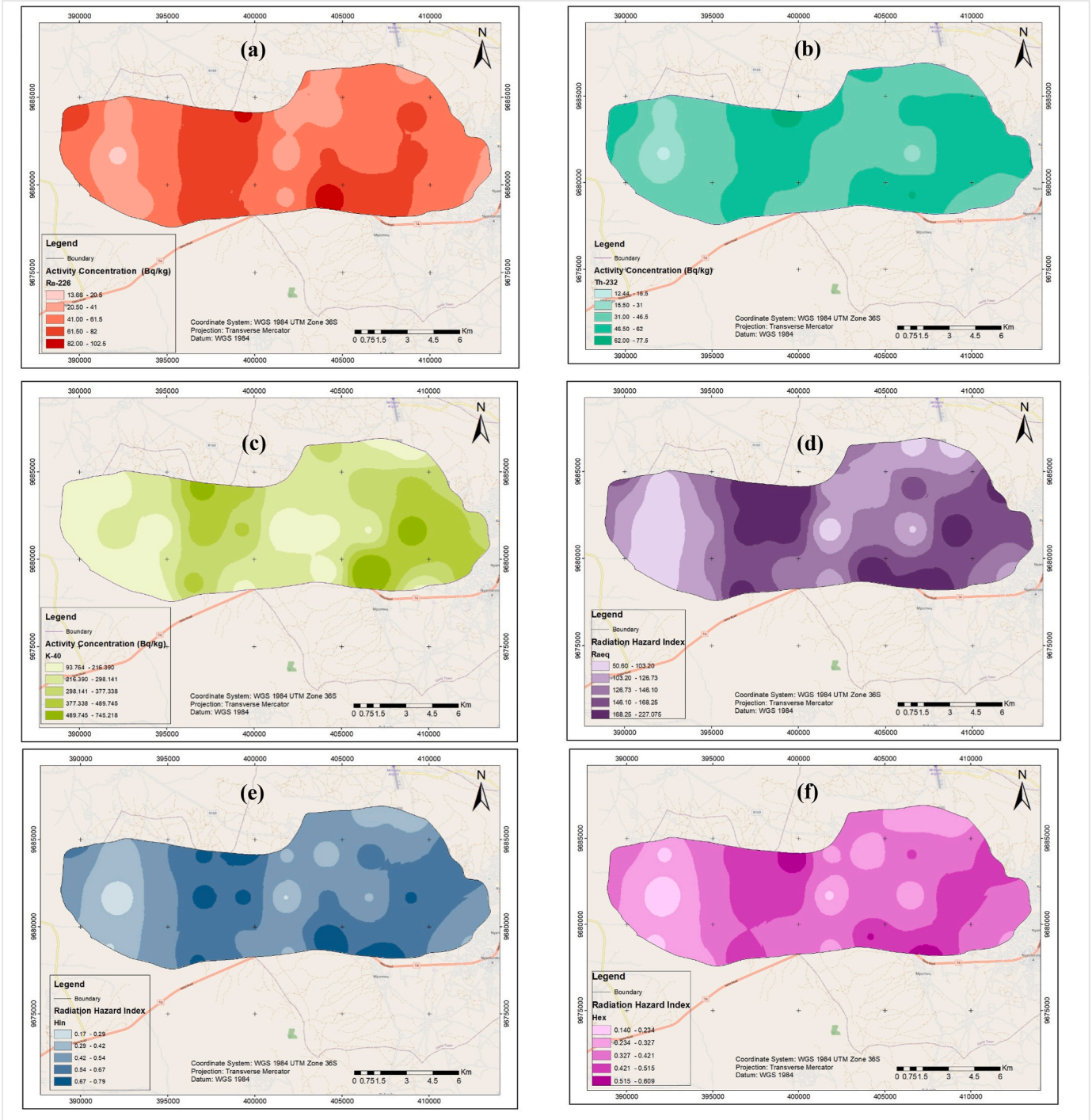

Fig. 3. Spatial distribution of the specific activity of (a) ^{226}Ra, (b) ^{232}Th, and (c) ^{40}K, and the radiation hazard indices (d) Ra_{eq}, (e) H_{ex}, and (f) H_{in}, around the Geita mining area.

10^{-3}, with an average of $(0.38 \pm 0.01) \times 10^{-3}$. The average ELCR obtained in this study is approximately 24 % higher than the global threshold of 0.29×10^{-3}, indicating elevated potential cancer risk from long-term exposure. The ECLR is about 75 % lower than the value of 1.5×10^{-3} reported at the Mashonga gold mine in Uganda (Silver et al., 2016). These findings reflect variability in radionuclide concentrations influenced by the local geological formations. They underscore the need to restrict the use of waste rocks as a construction material to mitigate potential long-term health risks.

3.9. Spatial distributions of the NORM across the mining area

The activity concentrations of ^{226}Ra, ^{232}Th, and ^{40}K exhibited notable spatial variability across the study area, reflecting the interplay of geological, environmental, and potentially anthropogenic factors. The highest activity concentrations of ^{226}Ra were observed in areas with specific activity concentrations of 82–102 Bq kg^{-1} displayed in darker red patches (Fig. 3(a)). These elevated levels may be linked to radium-enriched geological formations in this region, potentially influenced by uranium-bearing minerals that decay to produce radium (Kwelwa et al., 2018). The activity levels of ^{232}Th showed significant spatial

Table 11
Pearson correlation analysis between the calculated radiation hazard indices.

	^{232}Ra	^{232}Th	^{40}K	Ra_{eq}	H_{in}	H_{ex}	I_γ	AUI	D_R	AEDE	AGDE
^{232}Ra	1										
^{232}Th	0.554[a]	1									
^{40}K	0.427[a]	0.282	1								
Ra_{eq}	0.838[a]	0.762[a]	0.690[a]	1							
H_{in}	0.795[a]	0.578[a]	0.663[a]	0.862[a]	1						
H_{ext}	0.882[a]	0.589[a]	0.608[a]	0.884[a]	0.986[a]	1					
I_γ	0.772[a]	0.554[a]	0.701[a]	0.855[a]	0.997[a]	0.977[a]	1				
AUI	0.445[a]	0.414[a]	0.359*	0.480[a]	0.417[a]	0.433[a]	0.411[a]	1			
D_R	0.002	−0.094	0.124	−0.033	0.135	0.107	0.136	0.292	1		
AEDE	0.650[a]	0.396*	0.850[a]	0.755[a]	0.875[a]	0.844[a]	0.891[a]	0.400[a]	0.306	1	
AGDE	0.818[a]	0.695[a]	0.687[a]	0.945[a]	0.794[a]	0.825[a]	0.791[a]	0.491[a]	−0.059	0.712[a]	1

[a] Correlation is significant at the 0.01 level (2-tailed). *Correlation is significant at the 0.05 level (2-tailed).

variation, with the activity level 62–77 Bq kg^{-1} displaying the highest concentrations, as highlighted by the darker green patches (Fig. 3(b)). The localized enrichment in thorium could also result from geological factors, such as the presence of igneous rocks. For ^{40}K, the highest concentrations of 489–745 Bq kg^{-1} were observed in the dark light green patches (Fig. 3(c)). A distinct west-to-east concentration gradient was noted, likely reflecting the influence of potassium-rich feldspar minerals in the bedrock. The distribution of ^{40}K suggests a direct link to the region's geological characteristics, making it a valuable marker for underlying lithology.

The levels of Ra_{eq} exhibited wide spatial variability, with the highest values ranging from 168 to 227 as indicated by the darker purple shades (Fig. 3(d)). This pattern aligns with the elevated levels of ^{226}Ra and ^{232}Th in these regions. Conversely, lower Ra_{eq} values were observed in the western parts, characterized by lighter purple shades (Fig. 3(d)). This uneven distribution, with clusters of higher and lower values, indicates localized sources of radionuclides rather than a uniform gradient. The levels of H_{ex} and H_{in}, which represent the external and internal radiation hazards, respectively, varied spatially. The lowest values were found in the western and central part of the study area (Fig. 3(e) and (f)), correlating with the elevated levels of ^{226}Ra and ^{232}Th.

The spatial variability in radionuclide activity concentrations and associated indices emphasizes the influence of underlying geology, such as potassium-rich bedrock and thorium-bearing formations, as well as potential anthropogenic contributions. The clustering of high and low values underscores the need for localized environmental monitoring and radiological risk assessments. These findings are critical for guiding land use, public health measures, and sustainable resource management in the region.

3.10. Pearson correlation coefficient results

The correlation analysis was carried out as a bivariate statistic to determine the mutual relationships and strength of association between pairs of variables through the linear correlation coefficients. The results of the Pearson coefficients are shown in Table 11.

In this study, the terms 'strong', 'moderate', and 'weak' as applied to correlation coefficients refer to absolute coefficient values of >0.75, 0.75–0.50 and 0.50–0.36, respectively (Tanasković, Golobocanin, & Miljević, 2012). A moderate positive correlation is observed between ^{226}Ra and ^{232}Th (r = 0.554) because the uranium and thorium decay series exist together (Chandrasekaran et al., 2014; Tanasković, Golobocanin, & Miljević, 2012) and while a weak correlation was observed between ^{232}Th and ^{40}K (r = 0.427). A positive correction was observed for the Ra_{eq}, with ^{232}Ra, ^{232}Th, H_{ex}, H_{in}, I_γ, AGDE and AEDE (r = 0.833, 0.762, 0.884, 0.862, 0.855, 0.945 and 0.755), respectively. H_{ex} has a strong positive correlation with H_{in} (r = 0.986) and I_γ (r = 0.977), indicating their close association as radiological hazard indices. A weak correlation was observed between AUI with ^{226}Ra, ^{232}Th, ^{40}K, Ra_{eq}, H_{ex} and H_{in}, AEDE, and AGDE (r = 0.445, 0.414, 0.359, 0.480, 0.417, 0.411, 0.400 and 0.491), respectively. A weak correlation was observed between D_R with all the radionuclides and radiological hazard indices.

3.11. One-way ANOVA test results

The one-way ANOVA results revealed statistically significant differences ($p < 0.05$) in radiological hazard indices among soil, tailings and waste rock samples, with tailings and waste rocks displaying notably higher values. Post-hoc analysis using the Games-Howell test further confirmed that tailings exhibited the highest radionuclide concentrations and radiation exposure risks, significantly differing from soil samples ($p < 0.001$). However, no significant difference was found in the D_R values ($p = 0.210$), suggesting that gamma radiation exposure risks remain relatively similar across the three sample types. This highlights the need for targeted risk mitigation strategies for tailings and waste rock disposal, considering their elevated radiological indices.

The post-hoc (Games-Howell) test was also applied to calculate the source of significant differences. The outcome of the test revealed that there was a statistically significant mean difference between soil and tailings of −50.04 ($p < 0.001$) and between soil and waste rocks of −59.65 ($p = 0.025$). This suggests that the measured tailings and waste rocks are significantly more radioactive than the soil. Importantly, there was no significant difference between the Ra_{eq} values of the tailings and those of the waste rocks ($p = 0.814$).

The H_{in} values were significantly lower in soil compared to tailings (mean difference = −0.137, $p < 0.001$). However, no significant differences were found between values for the soil and those of the waste rocks ($p = 0.126$) or between tailings and waste rocks ($p = 0.906$). This suggests that the mining process, particularly in tailings, leads to a higher concentration of ^{232}Th compared to soil, but waste rocks do not significantly contribute to this increase in activity.

The H_{ex} values were significantly lower in soil compared to tailings, with a mean difference of −0.175 ($p < 0.001$), indicating that tailings pose a higher external radiation hazard than soil. No significant difference was observed between soil and waste rocks ($p = 0.087$) or between tailings and waste rocks ($p = 0.929$).

Significant differences were found between soil and tailings (mean difference = −0.209, $p < 0.001$), with soil exhibiting lower representative gamma index values. This result suggests that tailings show higher levels of gamma radiation, indicating a higher potential radiological risk. Again, there were no significant differences observed between soil and waste rocks ($p = 0.129$), or between tailings and waste rocks ($p = 0.974$).

A significant difference was observed between soil and tailings, with tailings having an AUI (mean difference = −0.170, $p = 0.036$). However, no significant difference was found between soil and waste rocks ($p = 0.078$) or between tailings and waste rocks ($p = 0.453$). This suggests that the mining process increases the alpha uncertainty index, particularly in tailings, compared to soil. Tailings showed a significantly

higher gamma dose rate than soil (mean difference = −21.71, $p < 0.001$), while waste rocks did not show a significant difference from either soil or tailings ($p = 0.210$ and $p = 0.987$, respectively). This indicates that tailings are a major source of radiation exposure compared to soil, while waste rocks do not significantly contribute to radiation dose rates.

The comparison revealed that both tailings and waste rocks had significantly higher AEDE values compared to soil. Specifically, the mean difference between soil and tailings was −98.10 ($p < 0.001$), and between soil and waste rocks was −99.52 ($p = 0.017$). These findings suggest that tailings and waste rocks pose a greater radiological risk in terms of annual effective dose compared to soil. No significant difference was found between tailings and waste rocks ($p = 0.998$), indicating that both sources have similar radiological risks in terms of AEDE.

The AGDE was significantly higher in tailings compared to soil (mean difference = −33.44, $p < 0.001$). No significant differences were found between soil and waste rocks ($p = 0.195$) or between tailings and waste rocks ($p = 0.987$). This reinforces the conclusion that tailings pose a significantly higher gamma radiation risk compared to soil.

The radiological hazard indices measured in this study, including Ra_{eq}, H_{ex}, H_{in}, I_{γ}, D_R, AEDE and AGDE, consistently exhibited higher values in tailings compared to soil (Faanu et al., 2014). This indicates that gold mining tailings contain a significantly higher concentration of radionuclides, which may pose long-term risks to both human health and the environment if not properly managed. To mitigate these risks, mining companies and regulatory authorities should consider implementing stricter containment measures for tailings, including lined storage facilities and controlled disposal protocols (Dixon-Hardy & Matthew, 2007). Additionally, continuous environmental monitoring should be conducted to assess changes in radiation levels over time and initiate interventions if necessary (Tripathi, Sahoo, Jha, Khan, & Puranik, 2008). Furthermore, local communities should be educated on potential exposure risks and provided with guidelines on safe land use practices near mining areas.

4. Conclusions

Activity concentrations of ^{226}Ra, ^{232}Th and ^{40}K of soil, tailings and waste rock samples around the Geita Gold Mine (GGM) in Tanzania was determined using the gamma spectrometry. The average activity concentrations of ^{226}Ra in soil (54 ± 3 Bq kg^{-1}), tailings (70 ± 2 Bq kg^{-1}) and waste rocks (67 ± 1 Bq kg^{-1}), ^{232}Th in soil (45 ± 1), tailings (36 ± 2 Bq kg^{-1}), and waste rocks (73 ± 1 Bq kg^{-1}) were compared to the global averages of 45 Bq kg^{-1}, and ^{40}K soil (279 ± 1 Bq kg^{-1}), tailings (878 ± 80 Bq kg^{-1}) and waste rocks (661 ± 7 Bq kg^{-1}) compared to the global average value of 35 420 Bq kg^{-1}. The activity concentrations of ^{226}Ra and ^{40}K followed the trend: tailings > waste rocks > soil sample, while for ^{232}Th, the trend was waste rocks > soil > tailings. The study also revealed significant spatial variability in the activity concentrations of ^{226}Ra, ^{232}Th, and ^{40}K, as well as their associated radiological hazard indices across the study area. The highest activity levels of ^{226}Ra were observed in the northeastern part of the GGM, while the ^{232}Th concentrations were most elevated in the central and southeastern regions. For ^{40}K, the northeastern area displayed the highest concentrations, with a general gradient of increasing levels from west to east, most probably linked to potassium-rich feldspar bedrock.

The spatial distribution of the radium equivalent activity (Ra_{eq}) mirrored the variability in the radionuclide concentrations, with the highest values concentrated in the central and southeastern regions and lower values in the west and northeast. Similarly, the radiation hazard indices (H_{ex} and H_{in}) exhibited localized peaks in the northeastern corner, indicating potential zones of slightly increased radiological risk.

The uneven distribution patterns observed for radionuclides and their hazard indices emphasize the influence of underlying geology, with contributions from potassium-rich and thorium-bearing rocks. A strong correlation is observed between ^{226}Ra and ^{232}Th, while a weak correlation is observed between ^{40}K and ^{226}Ra as well as ^{232}Th. It is also found that a positive correlation exists between Ra_{eq} with all the radionuclides and the rest of the radiation hazard indices.

The findings indicate that while the radiological indices for soil samples remain below the average global values stipulated by UNSCEAR, waste rock samples exhibit elevated levels that slightly exceeded average global values. This suggests a potential long-term radiological health risk, particularly if these materials are used in construction or other human activities. To mitigate these risks, strict regulatory measures should be enforced to ensure proper disposal and containment of mining waste and tailings. Additionally, further environmental health impact assessments are recommended to evaluate long-term exposure risk for communities residing near the GGM.

CRediT authorship contribution statement

Jerome M. Mwimanzi: Writing – review & editing, Writing – original draft, Visualization, Validation, Methodology, Investigation, Formal analysis, Data curation, Conceptualization. **Nils H. Haneklaus:** Writing – review & editing, Supervision, Project administration, Investigation, Funding acquisition, Formal analysis, Data curation, Conceptualization. **Tomislav Bituh:** Writing – review & editing, Investigation, Formal analysis, Data curation. **Hendrik Brink:** Writing – review & editing, Investigation, Funding acquisition, Formal analysis, Data curation. **Katarzyna Kiegiel:** Writing – review & editing, Investigation, Formal analysis, Data curation. **Farida Lolila:** Writing – review & editing, Investigation, Formal analysis, Data curation. **Janeth J. Marwa:** Writing – review & editing, Investigation, Formal analysis, Data curation. **Mwemezi J. Rwiza:** Writing – review & editing, Supervision, Investigation, Formal analysis, Data curation, Conceptualization. **Kelvin M. Mtei:** Writing – review & editing, Supervision, Investigation, Formal analysis, Data curation, Conceptualization.

Acknowledgement

This work received support from Tanzania Atomic Energy Commission (TAEC) and the Austrian Federal Ministry of Education, Science and Research (BMBWF) through Austria's Agency for Education and Internationalization (OeAD) [Grant Numbers: Africa UniNet P058, APPEAR Project341, WTZ HR 14/2024 and PL 12/2024]. APPEAR is a programme of the Austrian Development Organization. This work was further supported by the European Union – Next Generation EU projects EBDIZ [Program Contract of December 8, 2023, Class: 643-02/23-01/00016, Reg. no. 533-03-23-0006],Part of this research was conducted within the facilities founded by European Regional Development Fund project KK.01.1.February 1, 0007 ″Research and Education Centre of Environmental Health and Radiation Protection – Reconstruction and Expansion of the Institute for Medical Research and Occupational Health."

References

Aborisade, M., Gbadebo, A., Adedeji, O., Okeyode, I., & Ajayi, O. (2018). Excess lifetime Cancer risk and Radiation Pollution hazard indices in rocks and soil of some selected mining sites in Nasarawa State, Nigeria. *Aegean Journal of Environmental Sciences, 3*(3), 1–18.

Adebiyi, F. M., Ore, O. T., Adeola, A. O., Durodola, S. S., Akeremale, O. F., Olubodun, K. O., & Akeremale, O. K. (2021). Occurrence and remediation of naturally occurring radioactive materials in Nigeria: A review. *Environmental Chemistry Letters, 19*(4), 3243–3262. https://doi.org/10.1007/s10311-021-01237-4.

Ademola, A. K., Bello, A. K., & Adejumobi, A. C. (2014). Determination of natural radioactivity and hazard in soil samples in and around gold mining area in Itagunmodi, south-western, Nigeria. *Journal of Radiation research and applied sciences, 7*(3), 249–255. https://doi.org/10.1016/j.jrras.2014.06.001.

Akpanowo, M. A., Umaru, I., Iyakwari, S., Joshua, E. O., Yusuf, S., & Ekong, G. B. (2020). Determination of natural radioactivity levels and radiological hazards in environmental samples from artisanal mining sites of Anka, North-West Nigeria. *Scientific African, 10*. https://doi.org/10.1016/j.sciaf.2020.e00561.

Alharbi, S. (2024). Naturally occurring radioactive material (NORM) in Saudi arabia: A review. *Journal of Radiation research and applied sciences, 17*(3), 100981. https://doi.org/10.1016/j.jrras.2024.100981.

Amodu, F. R., Ben, F., Ben-Festus, B. N., Olawale, O. K., & Edaogbogun, G. O. (2024). Assessing scalability of natural radionuclides and associated risks in soils from gold mining areas in iperindo, southwestern Nigeria. *Mining, Metallurgy and Exploration, 41*(2), 925–935. https://doi.org/10.1007/S42461-024-00946-Y/METRICS.

AngloGold, A. (2021). Mineral resource and ore reserve report 2021. https://www.aga-reports.com/21/.

Atipo, M., Olarinoye, O., & Awojoyogbe, B. (2020). Comparative analysis of NORM concentration in mineral soils and tailings from a tin-mine in Nigeria. *Environmental Earth Sciences, 79*, 394. https://doi.org/10.1007/s12665-020-09136-7.

Ayeni, D. A., & Adebiyi, F. M. (2022). Evaluation of natural radioactivity and radiation hazards of soils around petroleum products marketing company using gamma-ray spectrometry. *Tanzania Journal of Science, 48*(2), 304–312. https://doi.org/10.4314/tjs.v48i2.7.

Bamidele, L., & Edun, A. O. (2024). Determination of activity concentration and radiological risks from gold mine tailings around ilahun-ijesa in obokun local government, osun state, Nigeria. *Journal of Applied Sciences & Environmental Management, 28*(4), 993–997. https://doi.org/10.4314/jasem.v28i4.3.

Banzi, F. P., Msaki, P. K., & Mohammed, N. K. (2017). Assessment of natural radioactivity in soil and its contribution to population exposure in the vicinity of mkuju river uranium project in Tanzania. *Expert Opinion on Environmental Biology, 6*(1), 4-4 https://doi.org/10.4172/2325-9655.1000140.

Bello, S., Nasiru, R., Garba, N. N., & Adeyemo, D. J. (2019). The concentration of ^{40}K, ^{226}Ra and ^{232}Th in soil and associated radiological parameters of shanono and bagwai artisanal gold mining areas, Kano state. *Journal of Applied Sciences, 23*(9). https://doi.org/10.4314/jasem.v23i9.8.

Bhave, P. P., & Sadhwani, K. (2022). Sampling in environmental matrices: A critical review. *Environmental Forensics, 23*(1–2), 75–92. https://doi.org/10.1080/15275922.2021.1887971.

Chandrasekaran, A., Ravisankar, R., Senthilkumar, G., Thillaivelavan, K., Dhinakaran, B., Vijayagopal, P., … Venkatraman, B. (2014). Spatial distribution and lifetime cancer risk due to gamma radioactivity in Yelagiri Hills, Tamilnadu, India. *Egyptian Journal of Basic and Applied Sciences, 1*(1), 38–48. https://doi.org/10.1016/j.ejbas.2014.02.001.

Cimorelli, A., Perry, S., Venkatram, A., Weil, J., Paine, R., Wilson, R., Lee, R., Peters, W., Brode, R., & Paumier, J. (2004). *AERMOD: Description of model formulation* (Vol. 454, pp. 3–4). US Environmental Protection Agency. *Epa-*.

Darwish, D. A. E., Abul-Nasr, K. T. M., & El-Khayatt, A. M. (2015). The assessment of natural radioactivity and its associated radiological hazards and dose parameters in granite samples from South Sinai, Egypt. *Journal of Radiation research and applied sciences, 8*(1), 17–25. https://doi.org/10.1016/j.jrras.2014.10.003.

Dixon-Hardy, D. W. E., & Matthew, J. (2007). Guidelines and recommendations for the safe operation of tailings management facilities. *Environmental Engineering Science, 24*(5), 625–637. https://doi.org/10.1089/ees.2006.0133.

Doyi, I., Essumang, D. K., Dampare, S., Glover, E. T., & toxicology. (2016). Technologically enhanced naturally occurring radioactive materials (TENORM) in the oil and gas industry: A review. *Reviews of environmental contamination*, 107–119. https://doi.org/10.1007/398_2015_5005.

El Aref, M., et al. (2020). Mineral Resources in Egypt (I): Metallic Ores. In Z. Hamimi, A. El-Barkooky, J. Martínez Frías, H. Fritz, & Y. Abd El-Rahman (Eds.), *The Geology of Egypt. Regional Geology Reviews. Springer, Cham*. https://doi.org/10.1007/978-3-030-15265-9_14.

El-Gamal, A., Nasr, S., & El-Taher, A. (2007). Study of the spatial distribution of natural radioactivity in the upper Egypt Nile River sediments. *Radiation Measurements, 42*(3), 457–465. https://doi.org/10.1016/j.radmeas.2007.02.054.

Emel, J., Plisinski, J., & Rogan, J. (2014). Monitoring geomorphic and hydrologic change at mine sites using satellite imagery: The Geita Gold Mine in Tanzania. *Applied Geography, 54*, 243–249. https://doi.org/10.1016/j.apgeog.2014.07.009.

Faanu, A., Adukpo, O. K., Tettey-Larbi, L., Lawluvi, H., Kpeglo, D. O., Darko, E. O., … Agyeman, L. (2016). Natural radioactivity levels in soils, rocks and water at a mining concession of Perseus gold mine and surrounding towns in Central Region of Ghana. *SpringerPlus, 5*(1), 1–16. https://doi.org/10.1186/s40064-016-1716-5.

Faanu, A., Darko, E. O., & Ephraim, J. H. (2012). Determination of natural radioactivity and hazard in soil and rock samples in a mining area in Ghana. *West African Journal of Applied Ecology, 19*(1), 77–92. https://www.ajol.info/index.php/wajae/article/view/77568/68009.

Faanu, A., Ephraim, J. H., & Darko, E. O. (2011). Assessment of public exposure to naturally occurring radioactive materials from mining and mineral processing activities of Tarkwa Goldmine in Ghana. *Environmental Monitoring and Assessment, 180*(1–4), 15–29. https://doi.org/10.1007/s10661-010-1769-9.

Faanu, A., Lawluvi, H., Kpeglo, D. O., Darko, E. O., Emi-Reynolds, G., Awudu, A. R., … Kpodzro, R. (2014). Assessment of natural and anthropogenic radioactivity levels in soils, rocks and water in the vicinity of Chirano gold mine in Ghana. *Radiation Protection Dosimetry, 158*(1), 87–99. https://doi.org/10.1093/rpd/nct197.

Focus, E., Rwiza, M. J., Mohammed, N. K., & Banzi, F. P. (2021). The influence of gold mining on radioactivity of mining sites soil in Tanzania. *EQA - International Journal of Environmental Quality, 46*, 46–59. https://doi.org/10.6092/issn.2281-4485/13288.

Haneklaus, et al. (2024). Rare earth elements and uranium in Minjingu phosphate fertilizer products: Plant food for thought. *Resources, Conservation and Recycling, 207*, 107694. https://doi.org/10.1016/j.resconrec.2024.107694.

Henckel, J., Poulsen, K., Sharp, T., & Spora, P. (2016). Lake Victoria goldfields. *Episodes, 39*(2), 135–154.

IAEA. (2014). *Radiation protection and safety of radiation sources*. International Basic Safety Standards. *IAEA Safety Standards Series No. GSR Part 3*.

IAEA. (2022). *IAEA nuclear safety and security glossary*.

ICRP. (2007). *ICRP publication* (Vol. 103). https://icrp.org/docs/ICRP_Publication_103-Annals_of_the_ICRP_37(2-4)-Free_extract.pdf.

ICRP. (2019). *ICRP publication 142: Radiological protection from naturally occurring radioactive material (NORM) in industrial processes* (Vol. 48). SAGE Publications Ltd. https://doi.org/10.1177/0146645319874589.

Kamunda, C., Mathuthu, M., & Madhuku, M. (2016). An assessment of radiological hazards from gold mine tailings in the province of Gauteng in South Africa. *International Journal of Environmental Research and Public Health, 13*(1). https://doi.org/10.3390/ijerph13010138.

Kazoka, A. R., Mwalilino, J., & Mtoni, P. (2023). A radiological risk assessment of 226Ra, 228Ra and 40K isotopes in Tilapia fish and its granitic environment in singida municipality. *Tanzania, 4*, 540–551. https://doi.org/10.3390/earth4030028.

Khisa Wanyama, C., Wanjala Makokha, J., Masinde, F. W., & Matsitsi, S. M. (2020). Radiological assessment of the activity concentrations of 40 K, 232 Th, 238 U and exposure levels in the rosterman gold mine of lurambi area, western, Kenya. *International Journal of Research and Scientific Innovation (IJRSI), VII*. www.rsisinternational.org.

Kileo, A. A., Salama, A., Chuma, F., & Pantaleo, P. (2025). Evaluation of radioactivity concentration and radiological impact for a closed open pit gold mine. *Brazilian Journal of Radiation Sciences, 13*(1), e2548. https://doi.org/10.15392/2319-0612.2025.2548.

Kovler, K., Friedmann, H., Michalik, B., Schroeyers, W., Tsapalov, A., Antropov, S., … Nicolaides, D. (2017). Basic aspects of natural radioactivity. *Naturally Occurring Radioactive Materials in Construction: Integrating Radiation Protection in Reuse (COST Action Tu1301 NORM4BUILDING)*, 13–36. https://doi.org/10.1016/B978-0-08-102009-8.00003-7.

Kwelwa, S. D., Dirks, P. H. G. M., Sanislav, I. V., Blenkinsop, T., & Kolling, S. L. (2018). Archaean gold mineralization in an extensional setting: The structural history of the Kukuluma and Matandani deposits, Geita Greenstone Belt, Tanzania. *Minerals, 8*(4), 171-171 https://doi.org/10.3390/min8040171.

Lolila, F., & Mazunga, M. S. (2023). Measurements of natural radioactivity and evaluation of radiation hazard indices in soils around the Manyoni uranium deposit in Tanzania. *Journal of Radiation research and applied sciences, 16*(1), 100524. https://doi.org/10.1016/j.jrras.2023.100524.

Lolila, F., Mazunga, M., & Ndabeni, N. B. (2022). Baseline measurements of natural radioactivity around the manyoni uranium deposit (Tanzania): Selection of sampling points. *Menemui Matematik (Discovering Mathematics), 44*(2), 97–108.

Lu, H., Kim, D., Liu, H., Xia, T., Reichard, W., Rodgers, M. O., & Guensler, R. (2024). Sensitivity of AERMOD (V21112) RLINEXT dispersion model outputs by source type to variability in single noise barrier height and separation distance. *Atmospheric Pollution Research, 15*(12), 102318. https://doi.org/10.1016/j.apr.2024.102318.

Michalik, B., Dvorzhak, A., Pereira, R., et al. (2023). A methodology for the systematic identification of naturally occurring radioactive materials (NORM). *Science of the Total Environment, 881*, 163324. https://doi.org/10.1016/j.scitotenv.2023.163324.

Moshupya, P. M., Mohuba, S. C., Abiye, T. A., Korir, I., Nhleko, S., & Mkhosi, M. (2022). In situ determination of radioactivity levels and radiological doses in and around the gold mine tailing dams, Gauteng province, South Africa. *Minerals, 12*(10), 1295. https://doi.org/10.3390/min12101295.

Odelami, K. A., Oladipo, M. O. A., Onoja, M. A., Musa, Y., & Aremu, S. O. (2024). Assessment of radiological contamination due to gold mining in soil and food crops of Babban Tsauni, Gwagwalada, Nigeria. *Radiation Protection Dosimetry, 200*(20), 1961–1970. https://doi.org/10.1093/rpd/ncae207.

Olayemi, O. S., Alausa, S. K., Coker, J. O., & Olabamiji, A. O. (2024). Radiological assessment and potential health risks of tailings from Komu, southwestern Nigeria. *Nigerian Journal of Physics, 33*(1), 36–42. https://doi.org/10.62292/njp.v33i1.2024.193.

ORTEC. (2020). *GammaVision ® maestro-PRO ®*.

Osimobi, J. C., Avwiri, G. O., & Agbalagba, E. O. (2018). Radiometric and radiogenic heat evaluation of natural radioactivity in soil around solid minerals mining environment in South-Eastern Nigeria. *Environmental Processes, 5*, 859–877. https://doi.org/10.1007/s40710-018-0336-1.

Pappa, F. K., Tsabaris, C., Ioannidou, A., Patiris, D. L., Kaberi, H., Pashalidis, I., … Vlastou, R. (2016). Radioactivity and metal concentrations in marine sediments associated with mining activities in Ierissos Gulf, North Aegean Sea, Greece. *Applied Radiation and Isotopes, 116*, 22–33. https://doi.org/10.1016/j.apradiso.2016.07.006.

Rabuku, A. T. W., & Malik, A. Q. (2020). Natural radioactivity measurement of gold mine tailings in Vatukoula, Fiji Islands. *Renewable Energy and Environmental Sustainability, 5*. https://doi.org/10.1051/rees/2020005.

Reddy, K. U., Ningappa, C., & Sannappa, J. (2017). Natural radioactivity level in soils around Kolar Gold Fields, Kolar district, Karnataka, India. *Journal of Radioanalytical and Nuclear Chemistry, 314*, 2037–2045. https://doi.org/10.1007/s10967-017-5545-y.

Saleh, G. M., Emad, B. M., Kader, I. B. A., & Sakr, R. M. (2021). The possible source of uranium mineralization in felsic volcanic rocks, Eastern Desert, Egypt of the Arabian-Nubian Shield: Constraints from whole-rock geochemistry and spectrometric prospection. *Acta Geochimica, 40*, 819–845. https://doi.org/10.1007/s11631-021-00472-4.

Samafou, P., Daniel, B., Alexandre, N. E., Maleka, P., Ajani, M. B., Hazou, E., … Godfroy, K. N. M. (2023). Evaluation of radiological hazards due to natural radioactivity in soil samples collected in and around some gold mining areas of the Mayo-Kebbi region in Chad with statistical analyses. *Arabian Journal of Geosciences, 16*(10), 1–12, 2023 16:10 https://doi.org/10.1007/S12517-023-11668-8.

Sawe, S. F. (2023). *Levels of radon in soils of dodoma city, Central Tanzania* (Vol. 9, pp. 92–103). https://doi.org/10.26437/ajar.31.03.2023.06.

Silver, T. E. R., Jurua, E., Oriada, R., Mugaiga, A., & Enjiku, B. (2016). Determination of natural radioactivity levels due to mine tailings from selected mines in southwestern Uganda. *Journal of Environment and Earth Science, 6*(6), 2224–3216. www.iiste.org.

Silvester, S. A., Lowndes, I. S., & Hargreaves, D. M. (2009). A computational study of particulate emissions from an open pit quarry under neutral atmospheric conditions. *Atmospheric Environment, 43*(40), 6415–6424. https://doi.org/10.1016/j.atmosenv.2009.07.006.

Sumary, D. P., Raymond, J., Chacha, M., & Banzi, F. P. (2024). *Radioactivity and dose assessment of naturally occurring radionuclides in terrestrial environments and foodstuffs: A review of bahi district, Tanzania* (Vol. 34, pp. 1652–1663). https://doi.org/10.1080/09603123.2023.2234299.

Tanasković, I., Golobocanin, D., & Miljević, N. (2012). Multivariate statistical analysis of hydrochemical and radiological data of Serbian spa waters. *Journal of Geochemical Exploration, 112*, 226–234. https://doi.org/10.1016/j.gexplo.2011.08.014.

Taskin, H., Karavus, M., Ay, P., Topuzoglu, A., Hidiroglu, S., & Karahan, G. (2009). Radionuclide concentrations in soil and lifetime cancer risk due to gamma radioactivity in Kirklareli, Turkey. *Journal of Environmental Radioactivity, 100*(1), 49–53. https://doi.org/10.1016/j.jenvrad.2008.10.012.

Tripathi, R., Sahoo, S., Jha, V., Khan, A., & Puranik, V. (2008). Assessment of environmental radioactivity at uranium mining, processing and tailings management facility at Jaduguda, India. *Applied Radiation and Isotopes, 66*(11), 1666–1670. https://doi.org/10.1016/j.apradiso.2007.12.019.

Tufail, M. (2012). Radium equivalent activity in the light of UNSCEAR report. *Environmental Monitoring and Assessment, 184*(9), 5663–5667. https://doi.org/10.1007/s10661-011-2370-6.

Tunde Ogundele, L., Oladotun, O. A., Abimbola, O. C., Samuel, & Inuyomi, O. (2021). Heavy metals, radionuclides activity and mineralogy of soil samples from an artisanal gold mining site in Ile-Ife. *Nigeria: Implications on Human and Environmental, 80*(5), 202. Springer https://doi.org/10.1007/s12665-021-09494-w.

UNSCEAR. UNSCEAR 2019 Report: Sources, effects and risks of ionizing radiation. Scientific Annexes A and B. https://www.unscear.org/unscear/en/publications/2019.html.

UNSCEAR. (2020). *UNSCEAR 2019 Report: Sources, effects and risks of ionizing radiation. Scientific Annexes A and B, 120*. https://www.unscear.org/docs/publications/2019/UNSCEAR_2019_Report.pdf.

Yachiso, G. T., Chaubey, A. K., & Turi, B. (2023). Measurements of natural radionuclide levels and hazards in the Lega Dembi gold mine, Oromia, Ethiopia. *Isotopes in Environmental and Health Studies, 59*(4–6), 554–566. https://doi.org/10.1080/10256016.2023.2273287.

Zhang, X., Huang, S., Yang, S., Tu, R., & Jin, L. (2020). Safety assessment in road construction work system based on group AHP-PCA. *Mathematical Problems in Engineering*, 2020. https://doi.org/10.1155/2020/6210569.